ISSN 1674-1056
http://cpb.iphy.ac.cn
http://iopscience.iop.org/cpb
中国物理 B
Chinese Physics
中国物理
Chinese Physics B

# Optical interaction between one-dimensional fiber photonic crystal microcavity and gold nanorod

Yang Yu(于洋), Ting-Hui Xiao(肖廷辉), Zhi-Yuan Li(李志远)
**Citation:**Chin. Phys. B . 2018, 27(1): 017301. **doi:** 10.1088/1674-1056/27/1/017301

Journal homepage: http://cpb.iphy.ac.cn; http://iopscience.iop.org/cpb

**What follows is a list of articles you may be interested in**

---

## Characteristics and mechanism analysis of Fano resonances in Π-shaped gold nano-trimer

Han-Hua Zhong(钟汉华), Jian-Hong Zhou(周见红), Chen-Jie Gu(顾辰杰), Mian Wang(王勉), Yun-Tuan Fang(方云团), Tian Xu(许田), Jun Zhou(周骏)
Chin. Phys. B . 2017, 26(12): 127301. **doi:** 10.1088/1674-1056/26/12/127301

## Tunable multiple plasmon resonances and local field enhancement of nanocrescent/nanoring structure

Wang Bin-Bing, Zhou Jun, Chen Dong, Fang Yun-Tuan, Chen Ming-Yang
Chin. Phys. B . 2015, 24(8): 087301. **doi:** 10.1088/1674-1056/24/8/087301

## Deep-ultraviolet surface plasmon resonance of Al and $Al_{core}/Al_2O_{3shell}$ nanosphere dimers for surface-enhanced spectroscopy

Ci Xue-Ting, Wu Bo-Tao, Song Min, Chen Geng-Xu, Liu Yan, Wu E, Zeng He-Ping
Chin. Phys. B . 2014, 23(9): 097303. **doi:** 10.1088/1674-1056/23/9/097303

## Fano-like resonance characteristics of asymmetric $Fe_2O_3$@Au core/shell nanorice dimer

Wang Bin-Bing, Zhou Jun, Zhang Hao-Peng, Chen Jin-Ping
Chin. Phys. B . 2014, 23(8): 087303. **doi:** 10.1088/1674-1056/23/8/087303

## High-order plasmon resonances in an Ag/$Al_2O_3$ core/shell nanorice

Chen Li, Wei Hong, Chen Ke-Qiu, Xu Hong-Xing
Chin. Phys. B . 2014, 23(2): 027303. **doi:** 10.1088/1674-1056/23/2/027303

---

# Optical interaction between one-dimensional fiber photonic crystal microcavity and gold nanorod*

Yang Yu(于洋)[1,2], Ting-Hui Xiao(肖廷辉)[1], and Zhi-Yuan Li(李志远)[1,3,†]

[1] *Laboratory of Optical Physics, Institute of Physics, Chinese Academy of Sciences, Beijing* 100190, *China*
[2] *University of Chinese Academy of Sciences, Beijing* 100049, *China*
[3] *School of Physics and Optoelectronics, South China University of Technology, Guangzhou* 510640, *China*

(Received 10 August 2017; revised manuscript received 26 September 2017; published online 17 November 2017)

Localized surface plasmon resonance (LSPR) has demonstrated its promising capability for biochemical sensing and surface-enhanced spectroscopy applications. However, harnessing LSPR for remote sensing and spectroscopy applications remains a challenge due to the difficulty in realizing a configuration compatible with the current optical communication system. Here, we propose and theoretically investigate a hybrid plasmonic-photonic device comprised of a single gold nanorod and an optical fiber-based one-dimensional photonic crystal microcavity, which can be integrated with the optical communication system without insertion loss. The line width of the LSPR, as a crucial indicator that determines the performances for various applications, is narrowed by the cavity–plasmon coupling in our device. Our device provides a promising alternative to exploit the LSPR for high-performance remote sensing and spectroscopy applications.

**Keywords:** photonic microcavtiy, localized surface plasmon resonance

**PACS:** 73.20.Mf, 42.82.Fv, 52.65.Ww, 78.67.Pt **DOI:** 10.1088/1674-1056/27/1/017301

## 1. Introduction

Localized surface plasmon resonance (LSPR), as a kind of coherent oscillation of the surface conduction electrons associated with optical polarization,[1–7] is capable of achieving strong enhancement and subwavelength confinement of electromagnetic fields. This offers the possibility to efficiently realize the strong light–matter interaction in the micro/nanoscales, which enables a variety of intriguing applications, such as biochemical sensing,[8–15] surface-enhanced spectroscopies,[16–20] nanolithographic fabrication,[21–25] and subwavelength photonic devices.[26–28]

Among various applications of LSPR, the line width of LSPR is a crucial indicator of the performance as it is closely related to the field enhancement and plasmon lifetime.[29] Due to the strong intrinsic material absorption, most LSPR line widths of metallic nanoparticles are confined to tens of nanometers, severely limiting the LSPR performance. To narrow the line width of LSPR, many structures and strategies have been explored, such as utilizing nanoparticle clusters to form steep Fano resonance line shapes[30–32] and coupling LSPR nanoparticles with high-quality photonic cavities.[4,26,33–36] However, making use of LSPR with a narrowed line width for remote sensing and spectroscopy applications remains a challenge due to the difficulty in realizing a configuration compatible with the current optical communication system and free from high coupling or insertion loss.

In this paper, we theoretically propose and investigate a hybrid plasmonic-photonic device for remote sensing and spectroscopy applications by coupling a single gold nanorod with an optical fiber-based photonic crystal microcavity. The whole configuration is designed within an optical fiber, which overcomes the difficulty of integrating with the optical communication system and avoids the high coupling or insertion loss. The dependences of the device performance on the cavity length, position and orientation of the nanorod are simulated and analyzed. Our design provides a promising configuration compatible with the current optical communication system to exploit LSPR with a narrowed line width, which is applicable for remote sensing and spectroscopy applications.

## 2. Results and discussion

We firstly investigate a hybrid gold nanorod-microfiber coupling system as shown in Fig. 1(a). A single gold nanorod with a bottom radius of 8 nm and a length of 169 nm is adhered to the surface of a microfiber with a diameter of 1.7 μm that satisfies the single-mode condition. The microfiber is adiabatically tapered from a single-mode fiber within an optical communication system, which will not induce any coupling or insertion loss. A plane wave with the *x*-direction polarization, propagating vertically to the microfiber, is used to excite the LSPR of the hybrid system. The long axis of the Au nanorod is parallel to the polarization direction of the incident wave, ensuring the excitation of the longitudinal mode of the nanorod. The transmission spectrum from the ends of the microfiber is

*Project supported by the National Basic Research Program of China (Grant No. 2013CB632704) and the National Natural Science Foundation of China (Grant No. 11434017).

†Corresponding author. E-mail: phzyli@scut.edu.cn

© 2018 Chinese Physical Society and IOP Publishing Ltd 

illustrated in Fig. 1(c), which is the LSPR spectrum of the hybrid system. The LSPR spectrum of the system is nearly equal to that of a single gold nanorod placed on a silica slab whose resonance peak is at 1466.2 nm while the line width is around 60 nm. The electric field magnitude distribution of the cross section of the hybrid system at the wavelength of 1466.2 nm is demonstrated in Fig. 1(b). When the distance between the nanorod and the microfiber is gradually increased, not only the blue shift of the LSPR peak but also the decrease of the transmission intensity can be observed, as shown in Fig. 1(d). The blue shift is due to the decrease of the effective optical path of the LSPR mode, originating from the decrease of the surrounding effective refractive index when the distance between the nanorod and the microfiber increases. The decrease of the transmission spectrum results from the decrease of the coupling efficiency between the nanorod and microfiber by the evanescent field.

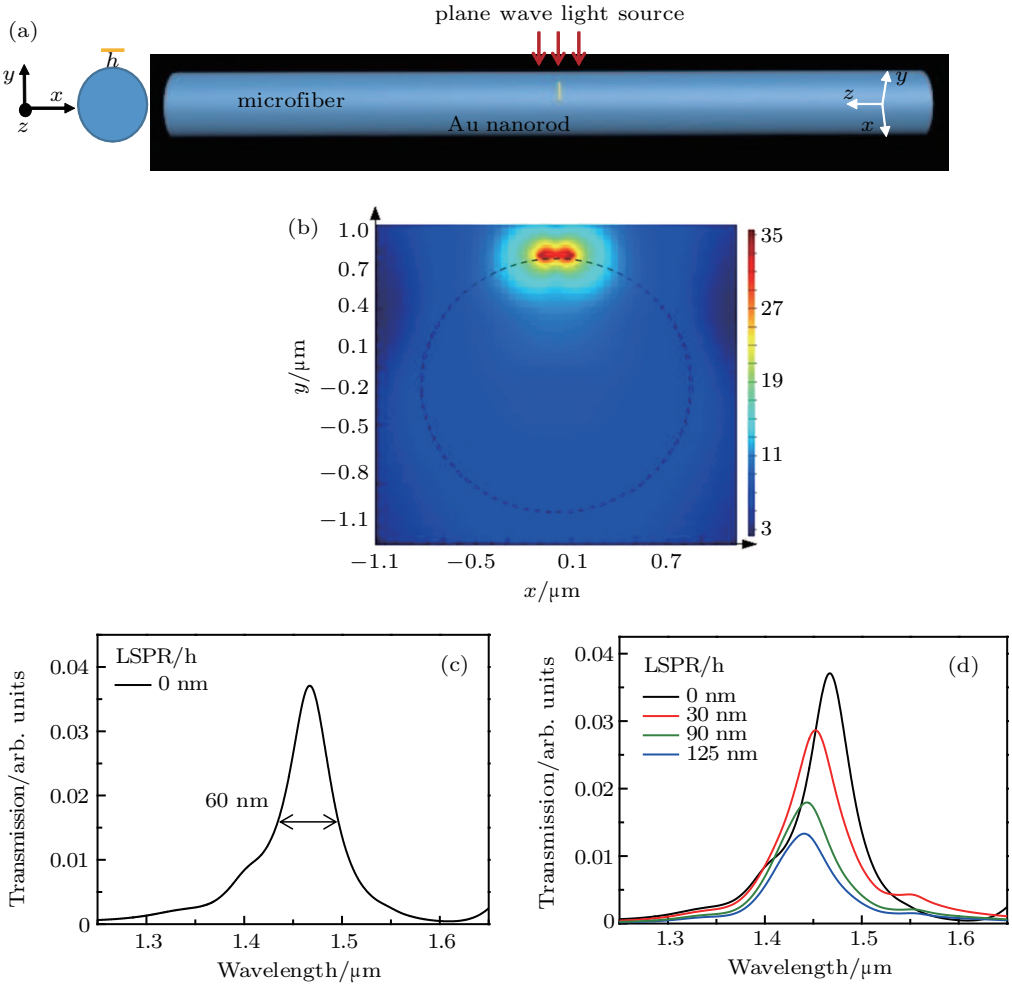



**Fig. 1.** (color online) (a) Hybrid gold nanorod-microfiber coupling system. (b) Electric field magnitude of the gold nanorod LSPR in the cross section of the system. (c) LSPR spectrum of the hybrid system with the nanorod being adhered to the surface of the microfiber. (d) Transmission spectrums with different distance $h$ between the nanorod and the microfiber surface.

With the above study as a basis and a comparison, we propose a hybrid plasmonic-photonic device comprised of a single gold nanorod and an optical fiber-based photonic crystal microcavity as shown in Fig. 2(a). The gold nanorod is integrated at a distance of 0.275 μm away from the center of the microcavity by adhering to the surface of the fiber. The designed microcavity whose cavity length is 0.9 μm consists of two broadband reflectors. Each reflector is an array of eleven $y$-direction through-holes with a period of 0.66 μm. The length and width of the through-holes are designed to be 1.2 μm and 0.3 μm, respectively, which not only ensures the bandgap of the reflector stays within the communication band but also makes the microcavity mechanically strong enough to be freely suspended.[37–39] When we excite the hybrid plasmonic-photonic device by an external $x$-polarized plane wave propagating vertically to the fiber as shown Fig. 2(a), the excited hybrid longitudinal mode in the $xz$ plane crossing the center of the microfiber is shown in Fig. 2(b). Due to the delicate design of the microcavity, the excited longitudinal mode is confined in an ultrasmall microcavity. The electric field strength at the center of the microfiber decays drastically along the $z$ axis into the mirror, revealing that the penetrating length of the reflector, through which the magnitude of the electric field decreases to $1/e$ of the original, is around four

periods. The transmission spectrum from the ends of the microfiber, which is the spectrum of the hybrid device, is illustrated by the solid line in Fig. 2(c). In comparison, the LSPR spectrum of a single nanorod is also shown by the dashed line in the figure. It is observed from the figure that the width of the resonance peak of the hybrid system is much smaller than that of a single nanorod even though both of them have the resonance peaks at the equal wavelength of 1466.2 nm. This is due to the coupling between the gold nanorod and the microcavity that greatly decreases the width of the resonance peak from 60 nm to 7.3 nm. As the width of the resonance peak is inversely proportional to the lifetime of photons oscillating in the resonant system, the decrease of the resonance peak width indicates the increase of the lifetime, which enhances the interaction between the oscillating photons and the surrounding environment of the device. The electric field magnitude of the cross section of our hybrid device is demonstrated in Fig. 2(d). The radiated photons of the LSPR of the gold nanorod will induce the excitation of the cavity mode, which goes back to further excite the LSPR.

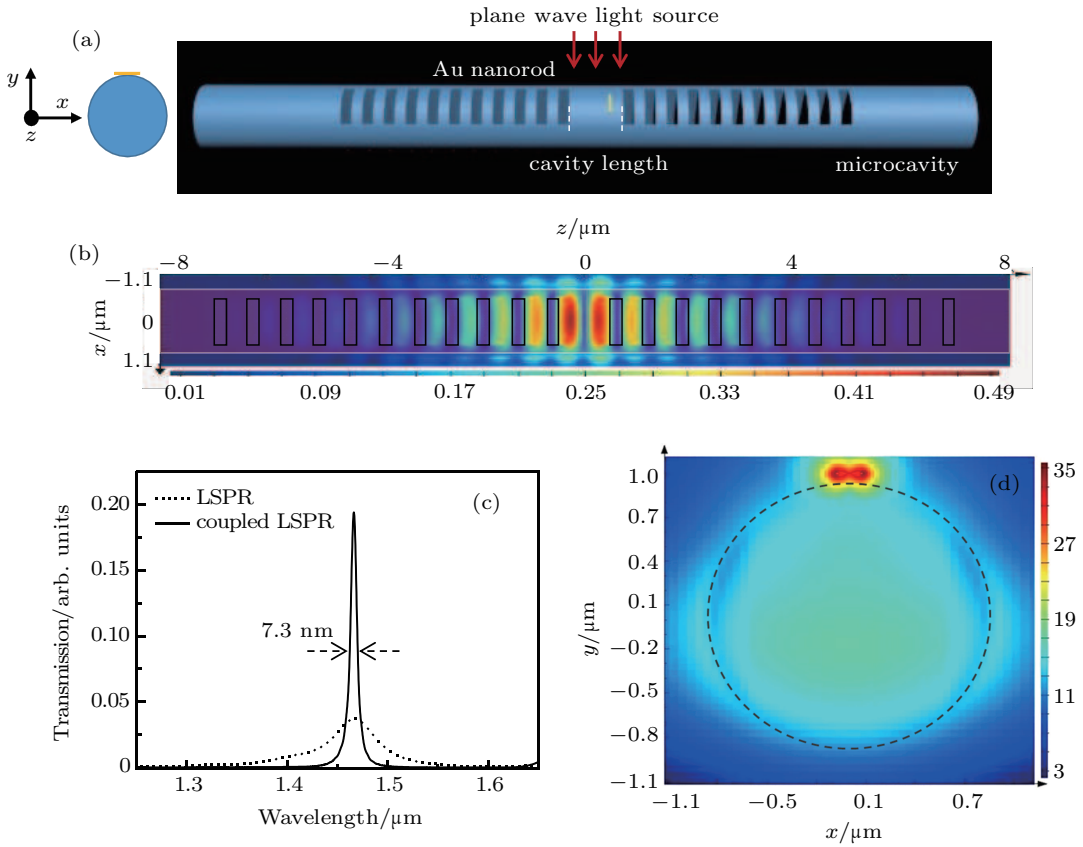



**Fig. 2.** (color online) (a) Hybrid plasmonic-photonic system. (b) Excited hybrid longitudinal mode in $xz$ plane crossing the center of the microfiber. (c) Spectrum of the hybrid system (solid line) and LSPR spectrum (dashed line). (d) Electric field magnitude in the cross section of the hybrid plasmonic-photonic device.

The dependence of the spectrum of our proposed device on the cavity length is studied as shown in Fig. 3. The dashed line depicts the LSPR spectrum of the gold nanorod while the solid lines represent the hybrid spectra of our device with different cavity lengths. It is observed that the transmission peak is the highest when the cavity length is 0.9 μm as shown by the black solid line. This is because the coupled light intensity into the microcavity is the highest when the resonance peak of the microcavity is coincident with that of the gold nanorod LSPR. Moreover, the coupling coefficient of the microcavity with the larger cavity length is higher than that with the smaller cavity length. For example, even though the radiation intensities of the LSPR are equal at the wavelengths of the resonance peaks of the hybrid devices with the cavity lengths of 0.94 μm and 0.86 μm respectively, the transmission intensity of the device with the cavity length of 0.94 μm is higher than that with the cavity length of 0.86 μm. This is because the increase of the cavity length increases the quality factor of the cavity, a critical parameter of the coupling condition, leading to the enhancement of the coupling from the LSPR radiation to the microcavity resonance. This demonstrates the tunability of the hybrid mode of our device by varying the cavity length.

We also study the dependence of the spectrum of our hybrid device on the position of the nanorod. As we have to excite the longitudinal mode of the LSPR, the propagation direction of the incident wave needs to be vertical while the polarization of the incident wave needs to be parallel to the long axis of the nanorod direction. Two different positions of the nanorod of our hybrid device are schematically shown at the left top of Fig. 4(a). These two positions are selected for two

different polarized incident waves. The $x$-polarized incident light means that the polarization of the incident wave is parallel to the $x$ axis while the propagation direction is along the $-y$ axis. The $y$-polarized incident light is polarized in the direction of the $y$ axis while it propagates along the $-x$ axis. The transmission spectra of these two different hybrid devices are demonstrated in Fig. 4(a). The width of the resonance peak of the device with the $x$-polarized incident wave is much narrower than that with the $y$-polarized incident wave. As the microcavity is designed for the $x$-polarized light, the hybrid device with $x$-polarized incident wave suffers from much less radiation loss than that with the $y$-polarized incident wave, thus possessing a higher quality factor. Additionally, compared with the device with the $x$-polarized incident wave, the device with the $y$-polarized incident wave shifts the resonance peak to the red wavelength. This is because the effective mode index of the excited hybrid mode in the device with the $y$-polarized incident wave is bigger than that with the $x$-polarized incident wave, thus leading to the increase of the effective length of the cavity. The difference of the effective mode indices of these two devices is also reflected in the hybrid transverse mode distributions as illustrated in Figs. 4(b) and 4(c). Besides these two positions, we further investigate the spectrum dependence of the hybrid device on the nanorod position in between the two positions with both $x$- and $y$-polarized incident light. The spectra of the hybrid device for different positions with $x$- and $y$-polarized incident light are shown in Figs. 5(a) and 5(b). The insets indicate the specific positions of the nanorod by the position angles. It is observed from the figures that the transmission of the hybrid device drastically decreases with the increase of the position angle from 0° to 30°. However, when the position angle of the nanorod further increases from 30° to $90^0$, the variation of the transmission is small. This indicates that the excitation efficiency of the hybrid mode, which is closely related to the excitation of the LSPR longitudinal mode and the coupling between the nanorod and the microcavity, is more sensitive to the variation of the position angle when it is smaller than 30°.

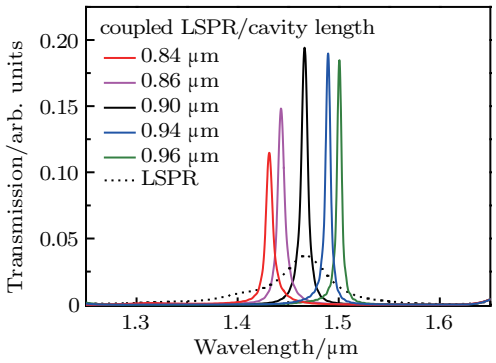



**Fig. 3.** (color online) LSPR spectrum (dashed line) and spectra of the hybrid plasmonic-photonic system with different microcavity lengths (solid lines).

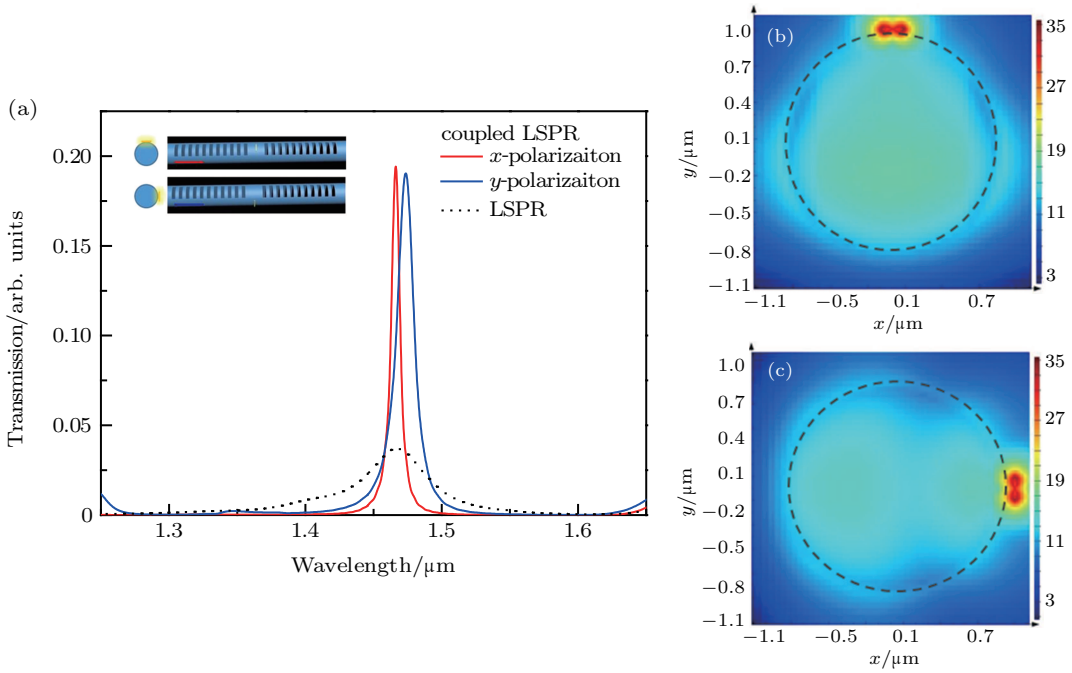



**Fig. 4.** (color online) (a) LSPR spectrum (the dashed line) and spectra of the hybrid plasmonic-photonic system with two vertical polarizations (solid lines). (b) Electric field magnitude of the hybrid device with the $x$-polarized incident wave. (c) Electric field magnitude of the hybrid device with $y$-polarized incident wave.

Furthermore, we investigate the dependence of the spectrum of our hybrid device on the orientation of the nanorod characterized by the angle $\theta$ (dashed arc line) as shown in Fig. 6(a). Figure 6(b) demonstrates the spectra of the hybrid device with different orientations. It can be observed that with the increase of the orientation angle, the transmission intensity of the device decreases dramatically. This is due to the decrease of the coupling coefficient originating from the varia-

tion of the polarization direction. The corresponding transmission intensities for different orientation angles are extracted and displayed in Fig. 6(c). The sensitivity of the transmission intensity to the variation of the orientation angle is larger from 2.5° to 5°. On the condition of $\theta$ being 0°, we further investigate the spectrum dependence of our hybrid device on the deviation of the nanorod from the center of the microcavity along the $z$ axis. Figure 7(a) shows the spectra of our hybrid device with the gold nanorod at different $z$ coordinates. With the increase of the $z$ coordinate of the nanorod, the transmission intensity of the device increases obviously. This is because the coupling increases with the increase of the electric field magnitude. When the gold nanorod arrives at the coordinate that is 0.275 μm away from the center of the microcavity, the electric field magnitude is the maximum as shown in Fig. 2(b), thus leading to the highest transmission intensity in Fig. 7(a). The corresponding transmission intensities for different deviations of gold nanorod are displayed in Fig. 7(b).

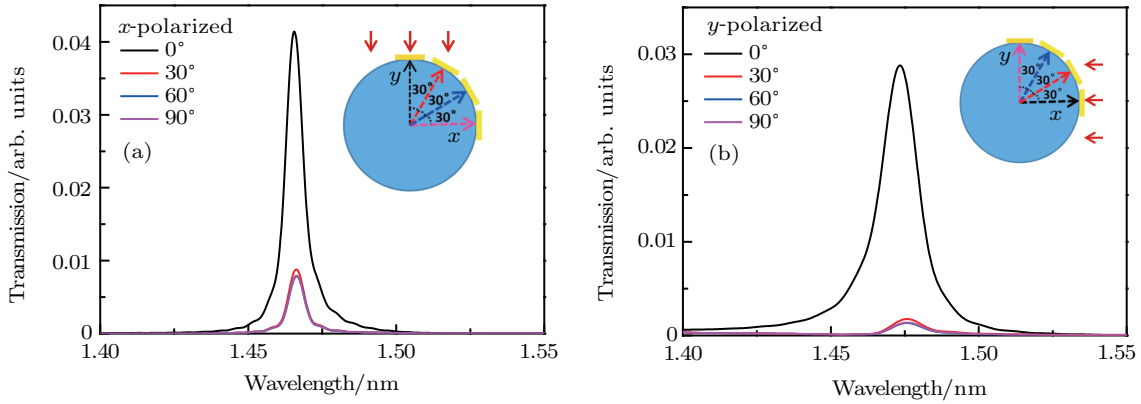



**Fig. 5.** (color online) Spectra of the hybrid plasmonic-photonic system with different position angles: (a) excited by $x$-polarized incident wave, (b) excited by $y$-polarized incident wave.

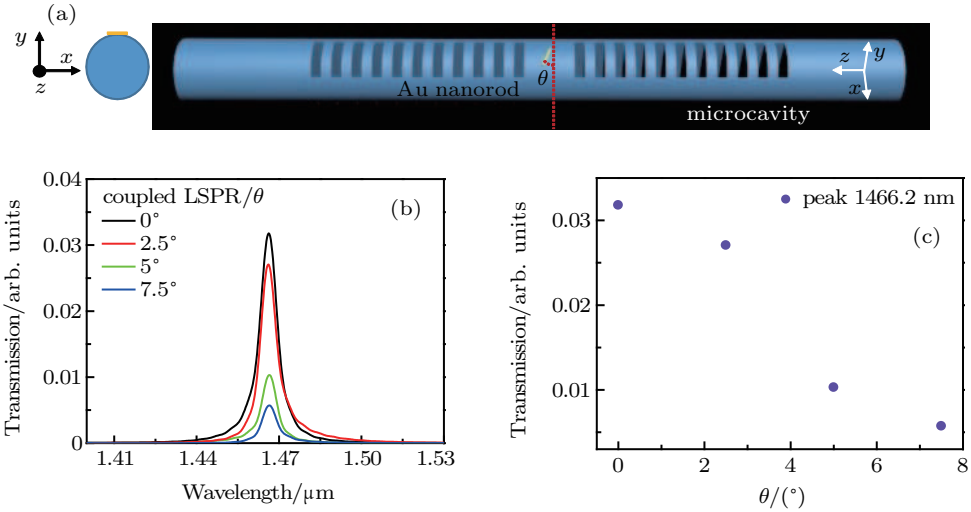



**Fig. 6.** (color online) (a) Hybrid plasmonic-photonic system with the nanorod orientation $\theta$. (b) Spectra of the hybrid device with different orientations from 0° to 7.5°. (c) The corresponding transmission intensities at the peak wavelength.

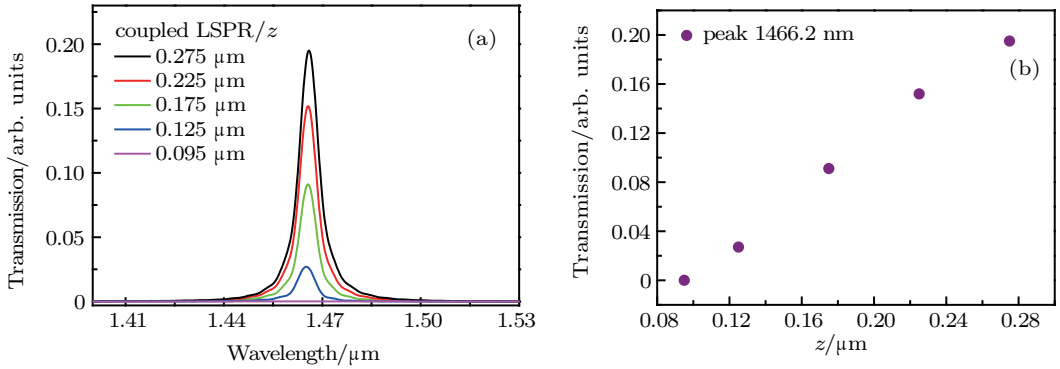



**Fig. 7.** (color online) (a) Spectra of the hybrid device with different deviations of the nanorod from the center of the microcavity. (b) Transmission intensities of the peak wavelengths with different deviations.

Based on the above investigation and analysis, we apply our device to refractive index sensing, as a proof of concept for its potential applications. The figure of merit (FOM) of our device, as a crucial parameter of a sensor that characterizes both the sensitivity and the sensing resolution,[9] is calculated and compared with the hybrid gold nanorod-microfiber coupling system. With the increase of the environmental refractive index from 1 to 1.04, the resonance peaks in both configurations experience red shifts as shown in Figs. 8(a) and 8(b). The FOMs of both configurations are calculated based on the specific red shifts and line widths. Our hybrid device possesses a FOM of 73.3 while the hybrid gold nanorod-microfiber coupling system possesses a FOM of 18.8. The larger FOM indicates a superior performance of our device in the refractive index sensing application.

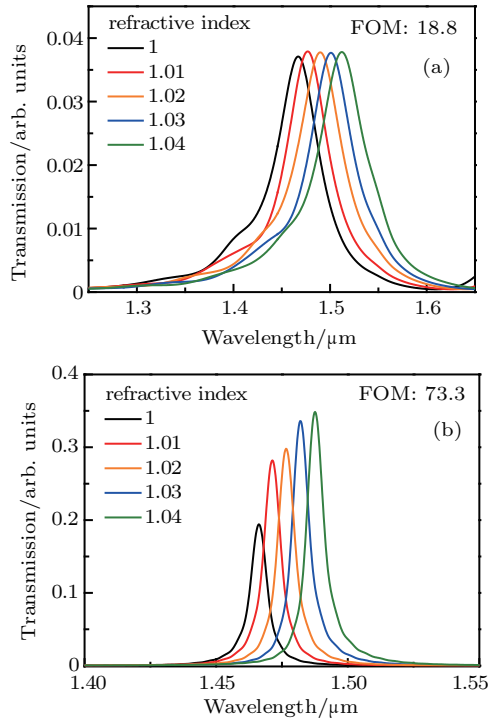



**Fig. 8.** (color online) (a) Spectra of the hybrid nanorod-microfiber coupling system with different environmental refractive indices. (b) Spectra of the hybrid plasmonic-photonic device with different environmental refractive indices.

## 3. Conclusion

In conclusion, we have theoretically proposed and investigated a hybrid plasmonic-photonic device comprised of a single gold nanorod and an optical fiber-based photonic crystal microcavity. Due to the coupling between the LSPR and the cavity mode, the line width of the LSPR, which is intimately related with the sensing resolution and plasmon lifetime, is narrowed from 60 nm to 7.3 nm. The dependence of the narrowed resonance peak on the cavity length, position and orientation of the nanorod are simulated and analyzed. Our device offers a promising alternative to overcome the difficulty of integrating LSPR with the current optical communication system for high-performance remote sensing and spectroscopy applications.

## References


[1] Eustis S and El-Sayed M A 2006 *Chem. Soc. Rev.* **35** 209
[2] Willets K A and Van Duyne 2007 *Rev. Phys. Chem.* **58** 267
[3] Bohren C F and Huffman D R 1983 *Absorption and Scattering of Light by Small Particles* (New York: Wiley) p. 3
[4] Wang P, Wang Y, Yang Z, Guo X, Lin X, Yu X C, Xiao Y F, Fang W, Zhang L, Lu G, Gong Q and Tong L 2015 *Nano Lett.* **15** 7581
[5] Kreibig U and Vollmer M 1995 *Optical Properties of Metal Clusters* (Berlin: Springer) pp. 1–12
[6] Sönichsen C, Franzl T, Wilk T, von Plessen G and Feldmann J 2002 *Phys. Rev. Lett.* **88** 077402
[7] Fang Z and Zhu X 2013 *Adv. Mater.* **25** 3840
[8] Anker J N, Hall W P, Lyandres O, Shah N C, Zhao J and Van Duyne 2008 *Nat. Mater.* **7** 442
[9] Mayer K M and Hafner J H 2011 *Chem. Rev.* **111** 3828
[10] Yonzon C R, Stuart D A, Zhang X, McFarland A D, Haynes C L and Van Duyne R P 2005 *Talanta* **67** 438
[11] Haes A J, Chang L, Klein W L and Van Duyne R P 2005 *J. Am. Chem. Soc.* **127** 2264
[12] Dahlin A B, Tegenfeldt J O and Hook F 2006 *Anal. Chem.* **78** 4416
[13] McFarland A D and Van Duyne R P 2003 *Nano Lett.* **3** 1057
[14] Raschke G, Kowarik S, Franzl T, Sonnichsen C, Klar T A and Feldmann J 2003 *Nano Lett.* **3** 935
[15] Elghanian R, Storhoff J J, Mucic R C, Letsinger R L and Mirkin C A 1997 *Science* **277** 1078
[16] Mühlschlegel P, Eisler H J, Martin O J F, Hecht B and Pohl D W 2005 *Science* **308** 1607
[17] Jeanmaire D L and Van Duyne R P 1997 *J. Electroanal. Chem.Interface Electrochem.* **84** 1
[18] Haynes C L, Yonzon C R, Zhang X and Van Duyne R P 2005 *J. Raman Spectrosc.* **36** 471
[19] Dieringer J A, McFarland A D, Shah N C, Stuart D A, Whitney A V, Yonzon C R, Young M A, Zhang X and Van Duyne R P 2006 *Faraday Discuss.* **132** 9
[20] Haller K L, Bumm L A, Altkorn R I, Zeman E J, Schatz G C and Vanduyne R P 1989 *J. Chem. Phys.* **90** 1237
[21] Noginov M A, Zhu G, Belgrave A M, Bakker R, Shalaev V M, Narimanov E E, Stout S, Herz E, Suteewong T and Wiesner U 2009 *Nature* **460** 1110
[22] Zhou W, Dridi M, Suh J. Y, Kim C H, Co D T, Wasielewski M R, Schatz G C and Odom T W 2013 *Nat. Nanotechnol.* **8** 506
[23] Fang N, Sun C, Luo Q and Zhang X 2004 *Nano Lett.* **4** 1085
[24] Kik P G, Maier S A and Atwater H A 2004 *Proc. SPIE* **5347** 215
[25] Sundaramurthy A, Schuck P J, Conley N R, Fromm D P, Kino G S and Moerner W E 2006 *Nano Lett.* **6** 355
[26] Chanda D, Shigeta K, Truong T, Lui E, Mihi A, Schulmerich M, Braun P V, Bhargava R and John A 2011 *Nat. Commun.* **2** 479
[27] Xiao T, Cheng Z and Goda K 2017 *Nanotechnology* **28** 245201
[28] Li Z, Li Y, Wang X, Yu Y, Tay B, Liu Z and Fang Z 2017 *ACS Nano* **11** 1165
[29] Yu Y, Ji Z, Zu S, Du B, Kang Y, Li Z, Zhou Z, Shi K and Fang Z 2016 *Adv. Funct. Mater.* **26** 6394
[30] Zhang S, Genov D A, Wang Y, Liu M and Zhang X 2008 *Phys. Rev. Lett.* **101** 047401
[31] Lassiter J B, Sobhani H, Fan J A, Kundu J, Capasso F, Nordlander P and Halas N J 2010 *Nano Lett.* **10** 3184
[32] Yanik A A, Cetin A E, Huang M, Artar A, Mousavi S H, Khanikaev A, Connor J H, Shvets G and Altug H 2011 *Proc. Natl. Acad. Sci. USA* **108** 11784
[33] Linden S, Kuhl J and Giessen H 2001 *Phys. Rev. Lett.* **86** 4688
[34] Christ A, Tikhodeev S G, Gippius N A, Kuhl J and Giessen H 2003 *Phys. Rev. Lett.* **91** 183901
[35] Ameling R, Langguth L, Hentschel M, Mesch M, Braun P V and Giessen H 2010 *Appl. Phys. Lett.* **97** 253116
[36] Kekatpure R D, Barnard E S, Cai W S and Brongersma M L 2010 *Phys. Rev. Lett.* **104** 243902
[37] Yu Y, W Ding, Li Z Y and Andrews S 2014 *Opt. Express* **22** 2528
[38] Yu Y, Sun Y Z, Andrews S, Li Z Y and Ding W 2015 *J.Phys.: Conf. Ser.* **680** 012029
[39] Yu Y, Xiao T H, Guo H L and Li Z Y 2017 *Photonic Research* **5** 143